International Journal of Advanced Engineering Research and Science (IJAERS)
Peer-Reviewed Journal
ISSN: 2349-6495(P) | 2456-1908(O)
Vol-12, Issue-5; May, 2025
Journal Home Page Available: https://ijaers.com/
Article DOI: *https://dx.doi.org/10.22161/ijaers.125.4*

Mathematical Modeling and Simulation of an Alkaline Electrolyzer for Hydrogen Production

Andrianaivoarivelo Jaolalaina Arisoa[1], Andrianjatovo Falinirina[2], Rafanjanirina Eulalie Odilette[3], Randriamanantany Zely Arivelo[4]

[1]Department of Physics, Faculty of Sciences, University of Antananarivo
jaolalaina@gmail.com, https://orcid.org/0009-0005-2323-2933
[2]Department of Physics, Faculty of Sciences, University of Antananarivo
afalinirina@gmail.com , https://orcid.org/0009-0009-0523-6788
[3]Department of Physics, Faculty of Sciences, University of Antananarivo
rafanjanirina@yahoo.fr
[4]Department of Physics, Faculty of Sciences, University of Antananarivo
zelyran@yahoo.fr

Received: 09 Apr 2025,

Receive in revised form: 07 May 2025,

Accepted: 13 May 2025,

Available online: 20 May 2025

©2025 The Author(s). Published by AI Publication. This is an open-access article under the CC BY license

***Keywords*— Green hydrogen, Alkaline electrolysis, Water electrolysis, Mathematical modeling, MATLAB/Simulink simulation, Electrolyzer performance, Ohmic loss and activation overpotential, Hydrogen production.**

***Abstract*—** *In the context of energy transition and the growing interest in green hydrogen as a sustainable fuel, this study presents a comprehensive mathematical modeling of an alkaline water electrolyzer. The paper investigates the fundamental physical and electrochemical processes involved in hydrogen generation, covering electric, thermodynamic, and electrochemical models. Key parameters such as electrolyte concentration, conductivity, membrane resistance, and gas bubble effects are incorporated. Simulation results using MATLAB/Simulink are provided to illustrate the behavior of the system under varying operational conditions. The findings contribute to the optimization of hydrogen production systems through accurate model-based design.*

I. INTRODUCTION

Hydrogen is increasingly recognized as a crucial pillar in the global transition toward a low-carbon energy future [1]. As countries and industries seek sustainable alternatives to fossil fuels, hydrogen stands out for its versatility, abundance, and clean combustion properties—producing only water vapor when used in fuel cells or combustion engines. Its application spans various sectors, including transportation, power generation, chemical manufacturing, and energy storage, making it a keystone for decarbonizing hard-to-abate industries and stabilizing renewable-dominated power grids [2].

A key determinant of hydrogen's environmental impact lies in the method of its production. Today, a significant portion of global hydrogen is still derived from fossil fuels, particularly through steam methane reforming (SMR), which results in substantial CO_2 emissions [3]. To achieve climate targets outlined in international agreements such as the Paris Accord, a paradigm shift toward low-emission or zero-emission hydrogen production is imperative. Among the various technologies available, water electrolysis emerges as a particularly promising solution, especially when powered by renewable electricity from solar, wind, hydro, or other sustainable sources. This method, often referred to as "green hydrogen" production, offers the potential for a

closed-loop energy cycle with minimal environmental footprint[4].

Water electrolysis involves the decomposition of water molecules (H_2O) into hydrogen (H_2) and oxygen (O_2) gases through the application of an electric current. Several electrolysis technologies have been developed over the years, including Proton Exchange Membrane (PEM) electrolysis, Solid Oxide Electrolysis (SOE), and Alkaline Water Electrolysis (AWE)[5] Among these, alkaline electrolysis remains one of the most mature and commercially viable options. It benefits from a long operational history, relatively simple system design, and the use of non-noble, low-cost catalysts such as nickel and iron-based materials. Furthermore, the scalability and reliability of AWE systems make them attractive for both centralized and decentralized hydrogen production facilities.

Despite its maturity, the alkaline electrolysis process presents several technical and scientific challenges that must be addressed to enhance efficiency, reduce capital and operational costs, and enable seamless integration into renewable energy systems [6]. Key areas of improvement include minimizing energy losses due to overpotentials, managing heat and mass transfer within the electrolyzer cell, and ensuring long-term stability under dynamic operating conditions. Achieving these objectives requires not only experimental advancements but also the development of accurate and comprehensive mathematical models capable of capturing the complex physical, chemical, and electrical behaviors of the system.

Modeling and simulation play a pivotal role in understanding and optimizing electrolyzer performance. By translating the underlying physical phenomena into mathematical expressions, models allow for predictive analysis, system design, sensitivity studies, and control strategy development. In the context of alkaline electrolysis, an effective model must integrate various interdependent domains: electrochemical kinetics governing the anode and cathode reactions, thermal dynamics affecting reaction rates and efficiency, and electrical parameters that determine cell voltage, current density distribution, and overall energy consumption [7].

This article presents a detailed and integrated mathematical model of an alkaline water electrolyzer. The model encompasses three key dimensions: electrical modeling, which establishes the relationship between applied voltage and current density while accounting for activation, ohmic, and concentration overpotentials; thermal modeling, which considers heat generation from internal resistances and electrochemical inefficiencies, along with heat dissipation via conduction, convection, and radiation; and electrochemical modeling, which describes the fundamental electrode reactions influenced by operating parameters such as electrolyte concentration, temperature, and pressure.

By simulating the behavior of the electrolyzer under various conditions—including different operating temperatures, current densities, and load profiles—the model provides critical insights into performance optimization. These simulations not only reveal the interplay between thermal and electrochemical dynamics but also highlight the impact of design choices on efficiency, hydrogen production rate, and operational stability.

Furthermore, the model has been implemented and validated using MATLAB/Simulink, offering a flexible framework for future expansion and integration into larger energy systems, such as hybrid renewable-hydrogen grids or sector-coupled infrastructures. Through parametric studies and sensitivity analyses, the model also facilitates informed decision-making for system design, control, and scaling.

II. ALKALINE ELECTROLYZER MODELING

2.1. Electrolyte Properties

In alkaline water electrolysis systems, the electrolyte serves as the primary medium for ionic conduction, bridging the electrochemical gap between the anode and cathode. Among various candidate electrolytes, potassium hydroxide (KOH) is most widely used due to its favorable properties, including high ionic conductivity, chemical stability, and compatibility with commonly used electrode materials. The hydroxide ions (OH^-) in the KOH solution are the primary charge carriers, moving from the cathode to the anode under the influence of an electric field. Their transport is essential for sustaining the redox reactions that occur at the electrodes: water is oxidized to oxygen at the anode, and reduced to hydrogen at the cathode. The ability of the electrolyte to facilitate efficient ion movement, while minimizing resistive losses, is central to the performance and energy efficiency of the electrolysis cell.

The physical properties of the KOH solution its concentration, density, ionic conductivity, and electrical resistance play critical roles in determining system behavior. These properties are not static; they evolve dynamically with changes in operating conditions, particularly temperature, electrolyte composition, and the presence of gas bubbles generated during electrolysis. To accurately simulate and predict the behavior of alkaline electrolyzers under real-world conditions, it is necessary to develop robust mathematical models that capture these

interdependencies with precision. Such models enable researchers and engineers to perform parametric studies, design optimization, and control strategy development for large-scale hydrogen production systems.

A fundamental quantity in electrolyte modeling is the molar concentration of KOH in the aqueous solution, which defines the number of moles of solute per liter of solution. In practice, commercial KOH solutions are typically described in terms of weight percentage (% w/w), which is more convenient for manufacturing and handling. However, physical and electrochemical models require molar concentration as input. Therefore, the first step in electrolyte characterization involves converting between weight percentage and molarity. This conversion depends on the density of the solution, which varies with both temperature and KOH concentration. The conversion is mathematically expressed as the equation (1):

$$C = \frac{10.\rho.\omega}{M} \quad (1)$$

where C is the molar concentration (mol/L), ω is the weight fraction (unitless), ρ is the density of the solution in g/cm³, and M is the molar mass of KOH (56.11 g/mol). Accurate calculation of C from www requires empirical correlations or tabulated data that provide solution density for various temperatures and concentrations. These correlations are typically derived from experimental measurements and interpolated to cover the desired operating range.

The density of the KOH solution itself is another crucial parameter, influencing not only the concentration conversion but also mass transport, buoyancy-driven convection, and hydrodynamic behavior within the cell. Density increases nonlinearly with concentration due to the progressive dissociation of KOH into K^+ and OH^- ions and their hydration by water molecules. However, the effect of temperature is inverse: as temperature increases, the kinetic energy of molecules disrupts hydrogen bonding and ionic hydration shells, leading to thermal expansion and reduced solution density. Empirical models typically represent density as a quadratic function of temperature at fixed concentrations, or as a surface fit over both variables equation (2).

$$\rho(T, C) = a + bT + cT^2 \quad (2)$$

where T is the temperature in °C, C is the molarity, and a, b, and c are empirically determined coefficients. Accurately modeling density is essential not only for thermodynamic calculations but also for determining natural convection currents and bubble rise velocities, which affect gas-liquid separation and mass transport within the cell.

Closely related to the density is the ionic conductivity of the KOH solution. This property defines the electrolyte's ability to transport charged species specifically, the hydroxide ions under an applied electric field. Conductivity depends strongly on both temperature and KOH concentration, and exhibits a non-linear behavior with respect to both. At low concentrations, increasing the KOH content leads to an increase in ion concentration and therefore higher conductivity. However, beyond a certain concentration (typically around 6 to 8 mol/L), conductivity reaches a peak and begins to decline. This is because the increased viscosity and interionic interactions at high concentrations impede ion mobility. Similarly, conductivity increases with temperature, as the thermal agitation enhances the diffusion coefficients of ions and reduces the solution's viscosity. This temperature effect can be modeled using Arrhenius-type equations or empirically fitted polynomial expressions. For instance, one widely used correlation is:

$$\kappa(T, C) = \kappa_0(C).[1 + \alpha(C)(T - T_0)] \quad (3)$$

where $\kappa(T, C)$ is the conductivity in S/m, κ_0 is the reference conductivity at a baseline temperature T_0, and is the temperature coefficient of conductivity, which varies with concentration. Accurate modeling of κ is essential for calculating ohmic losses in the cell and optimizing cell voltage for minimal energy consumption.

The electrical resistance of the electrolyte is inversely related to its conductivity and is governed by the classical formula (4):

$$R_{el} = \frac{d}{\kappa.A} \quad (5)$$

where R_{el} is the electrolyte resistance in ohms, d is the distance between electrodes, A is the cross-sectional area of conduction, and κ is the ionic conductivity. However, this expression assumes a homogenous medium, which is not the case during actual electrolysis, where gas bubbles of hydrogen and oxygen are continuously generated at the cathode and anode, respectively. These bubbles are non-conductive and occupy a fraction of the electrolyte's volume, thereby reducing the effective area available for ionic conduction. The presence of gas voids leads to increased local resistance and non-uniform current density distribution across the electrode surfaces. To account for this, the effective conductivity κ_{eff} is often modeled using Bruggeman's correction at the equation (6):

$$\kappa_{eff} = \kappa.(1 - \varepsilon)^n \quad (6)$$

where ε is the gas void fraction (volume of bubbles/total volume), and n is an empirical exponent typically ranging from 1.5 to 2.5 depending on the morphology of the bubbles. The void fraction itself depends on several factors including current density, surface roughness, electrode orientation, temperature, and pressure. High current densities generate more gas and lead to larger bubble formation rates, exacerbating the increase in resistance. Therefore, a comprehensive electrolyte model must dynamically update ε based on operating conditions to yield realistic resistance estimates.

In parallel to the electrolyte, the membrane in alkaline water electrolysis systems plays an equally pivotal role in determining the cell's performance, energy efficiency, and operational safety. While the electrolyte facilitates ionic conduction between the electrodes, the membrane physically separates the anode and cathode compartments, preventing the intermixing of hydrogen and oxygen gases while still permitting the transport of hydroxide ions (OH^-). This selective permeability is critical not only for product purity but also to avoid the formation of explosive gas mixtures. Moreover, the membrane contributes substantially to the overall cell resistance, as its microstructure and material composition directly influence the internal ohmic losses. Consequently, a detailed understanding of the membrane's physical characteristics and their influence on ionic conduction is essential for accurate electrochemical modeling and system design.

The effective performance of the membrane is governed by a combination of its chemical stability in caustic environments and its microstructural properties, including porosity, tortuosity, thickness, and surface area. Among these, porosity and tortuosity are particularly significant because they define the efficiency of ion transport through the membrane matrix. Porosity, typically expressed as a dimensionless volume fraction, represents the portion of the membrane that consists of interconnected voids or channels through which the electrolyte can diffuse. A higher porosity generally promotes greater ionic mobility by providing more conductive pathways, thereby decreasing internal resistance. However, excessive porosity can weaken the membrane mechanically or increase gas crossover, thereby compromising system reliability. Tortuosity, on the other hand, quantifies the geometric complexity of the ion transport paths. Even with high porosity, a highly tortuous structure can hinder effective ion conduction by increasing the actual distance that ions must travel, thus reducing the membrane's effective conductivity.

To model the impact of membrane structure on ionic transport, the effective conductivity σ_{eff} is commonly estimated using empirical or semi-empirical formulations that incorporate porosity **ε** and tortuosity **τ**. One of the most widely applied models is the Bruggeman correlation, which approximates effective conductivity as the equation (7):

$$\sigma_{eff} = \sigma_0 . \frac{\varepsilon}{\tau} \quad (7)$$

where σ_0 is the intrinsic conductivity of the bulk electrolyte (typically concentrated KOH), **ε** is the porosity, and **τ** is the tortuosity. This relationship reveals that even if the electrolyte is highly conductive, the microstructure of the membrane can significantly impede ion flow, thereby increasing the resistive losses within the cell. Both porosity and tortuosity are influenced by the membrane's fabrication method, aging, and the presence of fouling or gas bubble accumulation, all of which need to be considered in dynamic electrochemical models.

Temperature and electrolyte concentration further influence ionic conductivity, not just at the bulk electrolyte level but also within the membrane. As temperature increases, the viscosity of the KOH solution decreases and the mobility of hydroxide ions increases, which in turn enhances conductivity. However, the same temperature rise may also accelerate membrane degradation or increase gas permeability, which introduces trade-offs in design. Furthermore, the concentration of KOH impacts the number of available charge carriers, but only up to an optimal point beyond which ion pairing and viscosity effects begin to hinder transport. The conductivity behavior as a function of temperature and concentration within porous media follows similar nonlinear trends as observed in bulk solution but must be adjusted to reflect the microenvironment within the membrane.

From a structural perspective, the electrical resistance of the membrane is also a function of its thickness L and its effective surface area A. This relationship is captured by Ohm's law, equation (8), for a resistive medium:

$$R = \frac{L}{\sigma_{eff} \cdot A} \quad (8)$$

Here, increasing membrane thickness linearly increases resistance, while a larger active surface area contributes to lower resistance by distributing current over a broader region. In practical design, membrane thickness must be optimized to balance electrical performance with mechanical robustness. Thinner membranes typically offer lower resistance and thus lower voltage losses, but may be prone to rupture, delamination, or increased gas crossover under high-pressure operation. Surface area, in contrast, can be enhanced through the use of structured supports or flow field designs that increase membrane exposure without compromising integrity.

Over time, electrochemical operation can degrade membrane performance through physical wear, chemical attack, or deposition of impurities. These aging effects alter porosity, tortuosity, and mechanical strength, often resulting in increased resistance and reduced ionic selectivity. Models that predict long-term membrane behavior must therefore incorporate degradation kinetics and material fatigue, in addition to real-time operating parameters like current density, pressure, and electrolyte renewal rate. Moreover, the interaction of evolving gas bubbles with the membrane surface particularly under high current density can introduce non-uniformities in ion transport and localized resistance spikes.

To address the trade-offs inherent in membrane design, modern research is increasingly focused on composite and nanostructured membranes that combine desirable properties such as high ionic conductivity, mechanical strength, and chemical resistance. These include hybrid membranes incorporating inorganic fillers like zirconia or titania nanoparticles, which reduce tortuosity and enhance hydroxide ion pathways, as well as multilayer membranes that separate structural and transport functions. Such innovations aim to decouple conductivity from permeability and durability, pushing the boundaries of electrolysis efficiency.

Electrodes constitute the reactive interfaces where the core electrochemical transformations of water splitting occur—namely, the oxygen evolution reaction (OER) at the anode and the hydrogen evolution reaction (HER) at the cathode. In alkaline water electrolysis, the most commonly used electrode materials are based on nickel or nickel alloys due to their excellent catalytic activity in alkaline environments, mechanical robustness, relatively low cost, and compatibility with concentrated potassium hydroxide (KOH) electrolytes. The accurate modeling of electrode behavior is critical for predicting system efficiency, voltage requirements, and dynamic response to load variations. Electrode parameters influence not only the kinetics of charge transfer reactions but also the distribution of electric fields, current densities, and temperature gradients within the electrolyzer.

From an electrical standpoint, the electrodes must exhibit high intrinsic conductivity to minimize ohmic losses associated with in-plane and through-plane electron transport. The electrical conductivity (σ-e) of nickel-based materials typically ranges between 1×10^7 to 1.5×10^7 S/m at room temperature, depending on alloy composition and microstructure. Conversely, the resistivity (ρ_e), which is the reciprocal of conductivity, must be sufficiently low to ensure that current can be supplied to the electrochemical interface without significant voltage drop. The total resistive loss across an electrode, therefore, depends not only on the material's bulk resistivity but also on its geometric configuration (thickness and surface area), and its contact resistance with adjacent components such as the current collectors, porous transport layers, and the membrane.

Beyond their role as conductors, electrodes are sites of charge transfer where electrons from the external circuit interact with hydroxide ions and water molecules to drive the HER and OER. These interfacial processes are not instantaneous and involve overcoming energy barriers commonly referred to as activation overpotentials (η_{act}). Activation overpotentials represent the additional voltage required to surmount the kinetic limitations of the electrode reactions and initiate electron transfer. In electrochemical modeling, the Tafel approximation is often used to describe the nonlinear relationship between the overpotential and the resulting current density. For a single-step, rate-determining electrochemical reaction, the Tafel equation is given as the equation (9):

$$\eta_{act} = a + b.log_{10}(j) \quad (9)$$

where η_{act} is the activation overpotential (V), j is the current density (A/m²), a is the Tafel intercept (related to exchange current density), and b is the Tafel slope, which depends on temperature, number of electrons involved, and transfer coefficient. The slope b typically ranges between 30–120 $mV/decade$ for common alkaline reactions, and reflects the sensitivity of the reaction rate to applied overpotential.

The exchange current density j_0, embedded in the Tafel intercept, is a critical kinetic parameter that quantifies the intrinsic catalytic activity of the electrode material. It corresponds to the rate of the forward and reverse reactions at equilibrium (zero net current) and is strongly dependent on electrode surface area, morphology, electrolyte concentration, and temperature. For HER on nickel in alkaline media, j_0 values typically lie between 10^{-3} and 10^{-1} A/m², while for the more sluggish OER, values are generally lower, necessitating the use of dopants or composite materials like Ni-Fe or Ni-Co alloys to improve catalytic activity.

To improve overall performance, electrode surfaces are often engineered to increase the electrochemically active surface area (ECSA), which enhances the number of reactive sites and reduces the effective current density per unit area. This is achieved through techniques such as roughening, nanostructuring, or the use of porous and

foam-based substrates. The true current density, which affects reaction kinetics, must therefore be corrected for the real surface area rather than the geometric one, equation (10):

$$j_{real} = \frac{j_{geo}}{Ecsa/A_{geo}} \quad (10)$$

where j_{geo} is the measured current density based on geometric area A_{geo}, and $Ecsa$ is the electrochemically active surface area. Accurate modeling of activation losses requires realistic estimations of ECSA, which can be experimentally determined via cyclic voltammetry or impedance spectroscopy.

In addition to activation overpotentials, concentration overpotentials may arise due to mass transport limitations near the electrode surface, particularly at high current densities. Although these are typically less pronounced in well-mixed alkaline systems, their inclusion is essential for high-fidelity simulations. For porous electrodes, diffusion within the electrode matrix must also be considered, often modeled using the Nernst-Planck equation coupled with Darcy's law to capture electrochemical and fluid dynamic interactions.

Furthermore, the thermal and chemical stability of electrode materials under sustained operation is critical for long-term durability. High operating temperatures, aggressive chemical environments, and fluctuating loads can lead to corrosion, catalyst leaching, or changes in surface morphology, all of which degrade electrode performance over time. These degradation mechanisms can be incorporated into dynamic aging models, where parameters such as exchange current density and surface roughness evolve as functions of time, temperature, and electrochemical cycling.

In advanced models, the interfacial behavior of electrodes can also include double-layer capacitance and charge transfer resistance, which are particularly relevant for transient and impedance-based analyses. These components are typically represented in equivalent circuit models using resistor-capacitor (RC) networks and fitted to experimental electrochemical impedance spectroscopy (EIS) data.

2.2. Electrical and Electrochemical Model

Building upon the electrode-level phenomena described previously, the total cell voltage in an alkaline electrolyzer can be decomposed into a series of fundamental contributions that reflect the physical and electrochemical realities of water splitting. These include the reversible thermodynamic voltage, kinetic losses at the electrode interfaces, resistive losses across ionic and electronic conductors, and corrections for non-standard operating conditions. A comprehensive electrochemical model must capture these contributions to reliably simulate electrolyzer behavior under various load and environmental conditions.

At the core of this model lies the reversible cell voltage E_{rev} in equation 11, which represents the minimum theoretical voltage required to split water molecules under standard conditions (25°C, 1 atm, unit activity). It is determined from the Gibbs free energy change ΔG° of the overall electrochemical reaction. The reversible voltage serves as the thermodynamic lower limit for water electrolysis and is given by:

$$E_{rev} = \frac{\Delta G^{\circ}}{nF} \quad (11)$$

where n is the number of electrons transferred per molecule of H_2 (typically 2), and F is Faraday's constant. This value typically ranges around 1.23 V under standard conditions, but does not account for losses arising from electrode kinetics, transport resistances, or system configuration.

Superimposed on this ideal voltage are the ohmic losses V_{ohmic}, at the *equation 12*, which result from resistances encountered by both ionic and electronic charge carriers. These include the bulk electrolyte resistance (governed by KOH or NAOH concentration and temperature), the ionic resistance of the membrane, and resistive contributions from electrode contacts and gas bubbles formed at high current densities. The effective ohmic drop is calculated via:

$$V_{ohmic} = I.R_{total} = I.(R_e + R_m + R_b) \quad (12)$$

where R_e, R_m, and R_b are the resistances of the electrolyte, membrane, and gas bubble-induced blockage, respectively. These losses scale linearly with current and represent a significant portion of total voltage consumption, especially in high-efficiency systems operating at elevated currents.

Another major contributor to the cell voltage is the activation overpotential η_{act} (equation 13) at both the anode and cathode, arising from the finite rate of electrochemical reactions at the electrode-electrolyte interface. As outlined in *Section 2.3*, this kinetic barrier is typically modeled using the Tafel approximation, which links the overpotential to the logarithm of the current density:

$$\eta_{act} = a + b.\log(j) \quad (13)$$

These overpotentials differ significantly between the oxygen evolution reaction and hydrogen evolution

reaction, with oxygen evolution reaction typically being more sluggish and requiring higher overpotentials due to its complex, multi-electron transfer mechanism. The accurate estimation of these losses requires careful consideration of material-specific kinetic parameters such as the exchange current density and Tafel slope, both of which are sensitive to surface structure, temperature, and electrolyte composition.

To account for non-standard operating conditions, the cell voltage must also incorporate a Nernstian correction that adjusts the theoretical voltage to reflect actual partial pressures of hydrogen and oxygen, as well as hydroxide ion concentration. The Nernst *equation 14* provides this adjustment:

$$R_{Nerst} = E^o + \frac{RT}{nF}\ln\left(\frac{a_{product}}{a_{reactants}}\right) \quad (14)$$

Here, *R* is the universal gas constant, *T* is the absolute temperature, and *a* represents the activity (partial pressure) of the species involved. This correction is critical when simulating industrial conditions where pressures and concentrations differ significantly from standard-state assumptions.

Combining these contributions, the total operating cell voltage is expressed as the equation 15:

$$V_{cell} = E_{rev} + \eta_{anode} + \eta_{cathode} + V_{ohmic} + \Delta_{Nernst} \quad (15)$$

This expression forms the backbone of any predictive electrochemical model and allows for parametric studies on system performance as a function of material properties, current density, temperature, and electrolyte composition. The model can be further refined by incorporating temperature dependence of each term, dynamic behavior under load cycling, and degradation factors for long-term operation.

In conclusion, the electrical and electrochemical model serves as a critical extension of electrode-level analysis, integrating thermodynamic, kinetic, and transport phenomena to provide a full picture of voltage requirements and energy efficiency in alkaline electrolysis. Accurate representation of each component is essential for guiding the design of high-performance electrolyzers and enabling reliable techno-economic assessments.

2.3. Thermodynamic Model

The thermodynamic model underpins the fundamental energy requirements of water electrolysis by focusing on the intrinsic energetics of the water splitting reaction. Unlike the electrochemical model, which addresses the voltage losses associated with practical system components, the thermodynamic model isolates the ideal energy input based on changes in enthalpy (ΔH) and entropy (ΔS) associated with the reaction. These thermodynamic quantities define the energy content and disorder change as water molecules are dissociated into hydrogen and oxygen gases, and are crucial for understanding the theoretical efficiency limits of the electrolytic process.

At the heart of the thermodynamic model lies the distinction between the Gibbs free energy change (ΔG) and the enthalpy change (ΔH) of the reaction. The Gibbs free energy represents the minimum electrical work needed to split water under reversible, isothermal, and isobaric conditions, while the enthalpy encompasses the total energy, both electrical and thermal required to drive the reaction. The standard enthalpy change for the overall reaction (equation 16) at 25°C is approximately +285.8 kJ/mol, and the corresponding Gibbs free energy change is +237.2 kJ/mol[8]. These values demonstrate that a portion of the energy required for water electrolysis can be supplied as heat, especially under elevated temperature operations.

$$H_2O \rightarrow H_2 + \tfrac{1}{2}O_2 \quad (16)$$

This thermodynamic analysis leads to the concept of the thermoneutral voltage E_{th} in the equation 17, which represents the voltage at which the supplied electrical energy is exactly balanced by the total enthalpic demand of the reaction, without any net heat generation or absorption. The thermoneutral voltage is defined by:

$$E_{th} = \frac{\Delta H}{nF} \quad (17)$$

where ΔH is the enthalpy change per mole of reaction, n is the number of electrons transferred ($n = 2$ for hydrogen generation), and F is Faraday's constant. At standard conditions, E_{th} is approximately 1.48 V. This value is higher than the reversible voltage (typically $\approx 1.23\ V$), highlighting the gap between the minimum electrical input (from ΔG) and the total energy requirement (from ΔH), which can be partially compensated by thermal energy input in high-temperature systems.

The difference between the thermoneutral voltage and the reversible voltage provides a framework for evaluating the efficiency and energy integration potential of electrolyzer systems. Operating at voltages close to the thermoneutral value enables thermally balanced operation, where no excess heat is required or released, while operation below this value necessitates external heat input to sustain the reaction. Conversely, if the cell is operated above the thermoneutral voltage, excess heat is generated, which may require active cooling and presents opportunities for cogeneration or heat recovery.

Furthermore, temperature-dependent variations in ΔG and ΔH must be taken into account when modeling thermodynamic behavior across a range of operating temperatures. These dependencies influence both the thermodynamic efficiency and the practical feasibility of operating the system under non-standard conditions, such as in high-temperature electrolysis. The integration of these parameters into a comprehensive thermodynamic framework allows for accurate prediction of the energy flows in the system and supports the optimization of thermal and electrical input in hybrid energy scenarios.

The thermodynamic model provides essential insight into the fundamental energy landscape of water electrolysis by establishing the theoretical bounds of energy input based on enthalpy and entropy changes. The concept of the thermoneutral voltage bridges the gap between ideal reversible operation and real energy demands, forming a foundational element for the design, optimization, and thermal integration of advanced alkaline electrolyzer systems.

The hydrogen production rate is a central performance metric in electrolyzer operation, directly linking the applied electrical input to the chemical output. In alkaline electrolysis, the hydrogen molar flow rate $\dot{n}_{H_2}$ (equation 18) is governed by Faraday's law of electrolysis, which quantifies the amount of substance produced or consumed at an electrode as a function of the total charge passed through the system. This relationship provides a direct pathway to estimate the production capacity of the electrolyzer under varying operating conditions.

The molar flow rate of hydrogen is given by the following expression:

$$\dot{n}_{H_2} = \frac{n_F . I}{n . F} \qquad (18)$$

where:

$\dot{n}_{H_2}$ is the hydrogen molar flow rate (mol/s),

n_F is the Faradaic efficiency (dimensionless, 0–1),

I is the applied current (A),

n is the number of electrons per mole of hydrogen produced (n = 2),

F is Faraday's constant (≈96485C/mol).

Faradaic efficiency, n_F, equation 19 represents the fraction of the total electrical charge that effectively contributes to the desired hydrogen-producing reaction. In practice, side reactions and parasitic processes such as oxygen crossover, hydrogen back-diffusion, and gas bubble accumulation can reduce n_F, especially at elevated temperatures or high current densities.

To reflect these variations, n_F is often modeled as a temperature-dependent function. Empirical expressions or fitting curves derived from experimental data are used to correlate current efficiency with temperature (*T*), and sometimes with current density (*j*) and pressure (*P*). A commonly used form is:

$$\eta_F(T) = \eta_0 . \left(1 - \alpha . (T - T_0)\right) \qquad (19)$$

where:

η_0 is the reference Faradaic efficiency at temperature T_0,

α is a degradation K^{-1} indicating how quickly efficiency drops with temperature increase,

T is the actual operating temperature (K),

T_0 is the reference temperature, typically 298.15 K (25°C).

In high-performance systems where thermal management and gas-liquid separation are optimized, Faradaic efficiencies can approach 98–100%. However, even slight reductions in efficiency can significantly impact long-term hydrogen yield and energy conversion metrics, particularly in large-scale installations.

The hydrogen production rate can be converted into volumetric flow rate (equation 20) under standard conditions using the molar gas constant:

$$\dot{V}_{H_2} = \dot{n}_{H_2} . \frac{R T_{STP}}{P_{STP}} \qquad (20)$$

This allows the model to express outputs in units more commonly used in practical and industrial contexts, such as normal liters per minute (NL/min) or cubic meters per hour (Nm^3/h), facilitating integration with downstream storage, compression, or fuel cell subsystems.

The hydrogen production rate model establishes a direct quantitative connection between electrical input and hydrogen output, modulated by system efficiency and operational parameters. Accurately modeling this relationship especially with respect to current efficiency and temperature sensitivity is essential for optimizing electrolyzer design, predicting system throughput, and conducting meaningful techno-economic assessments in real-world applications.

III. SIMULATION AND RESULTS OF THE MODEL

Simulations were conducted to evaluate the influence of operational parameters on the electrical response during the startup phase of the electrolyzer. Several simulations were performed at various input voltages and temperatures. The purpose of these simulations was to observe the system's behavior under varying conditions. The simulation environment used for this analysis was MATLAB/SIMULINK®.

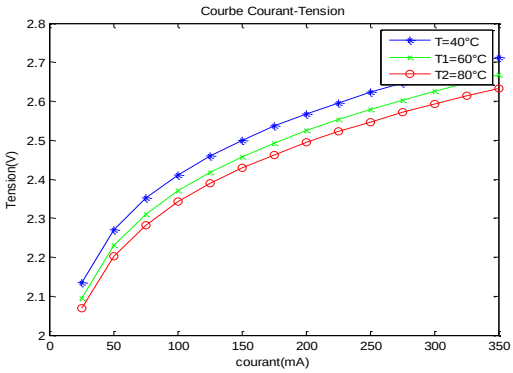

Fig.1: Voltage-current characteristic of an electrolyzer at 40°C, 60°C, and 80°C

Figure 1 illustrates how the operating voltage of an electrolyzer varies with both current and the temperature of the alkaline solution. As the current increases, the voltage also rises, reaching a quasi-stable value around 350 mA. The effect of temperature is clearly discernible, demonstrating its significant role in the electrochemical behavior of the cell. Specifically, the voltage and temperature exhibit an inverse relationship, which is a key finding for system optimization.

At lower temperatures, such as 40°C, the cell voltage reaches a maximum of approximately 2.7 V, whereas at higher temperatures, such as 80°C, the voltage drops to around 2.6 V. This behavior indicates that increasing the operating temperature reduces the internal resistance and activation overpotentials within the electrolyzer. Scientifically, this underscores the importance of thermal management in alkaline electrolysis systems to enhance performance and energy efficiency.

3.1. Voltage-Current Relationship

The reversible decomposition voltage of an electrochemical cell, defined as the minimum voltage required to initiate water electrolysis under standard conditions, is approximately 1.2 V. This value corresponds to the Gibbs free energy change of the water-splitting reaction. However, because the reaction is endothermic, with a reaction enthalpy of 282 kJ/mol, additional energy must be supplied to maintain the system's thermal balance. This leads to the concept of the thermo-neutral voltage, which is about 1.46 V. At this voltage, the electrolyzer operates without net heat absorption or release, ensuring stable temperature conditions during the electrolysis process.

In practical operation, the voltage applied across the cell must exceed the thermo-neutral value due to unavoidable losses. The actual cell voltage used in this case is 2.0 V, which accounts for several types of overpotentials and resistive effects. These contributions are expressed in the equation 21:

$$V_{cell} = V_{rev} + V_{ohmic} + V_{act} + V_{conc} \quad (21)$$

where V_{rev} is the reversible voltage, V_{ohmic} represents the ohmic losses through the electrolyte, membrane, and electrodes, V_{act} is the activation overpotential linked to the kinetics of the electrochemical reactions, and V_{conc} accounts for concentration polarization due to mass transport limitations.

To gain a deeper understanding of these voltage contributions, one can refer to the characteristic curves available in the "Profiles" section. These curves illustrate how each voltage component evolves with increasing current density, offering valuable insights into the internal processes of the electrolyzer. Such analysis is crucial for optimizing the design and performance of alkaline electrolyzers, as it highlights the trade-offs between efficiency, thermal management, and electrochemical kinetics. The evolution of cell voltage components as a function of current density is shown in figure 2.

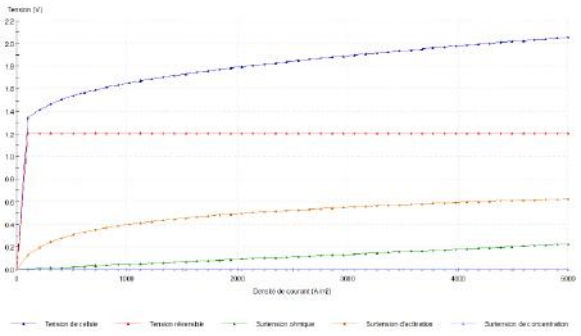

Fig.2: Evolution of cell voltage components as a function of current density

3.2. Sensitivity Analysis

A sensitivity analysis was carried out by varying the current density from 400 to 5000 A/m². To implement this variation, it was necessary to redefine the electrical current input in the "General" settings tab by selecting “Current Density” instead of total current. The minimum value of

current density was chosen to ensure that the electrolyzer operates above the thermoneutral voltage. This approach allows for a deeper understanding of how performance parameters evolve under different electrochemical loads, an important consideration for optimizing system design.

Figure 3 illustrates the variation of cell voltage and total electrical power consumption as a function of current density. This figure reveals that increasing current density leads to a nonlinear increase in both parameters, suggesting a significant rise in ohmic and overpotential losses at higher operating conditions.

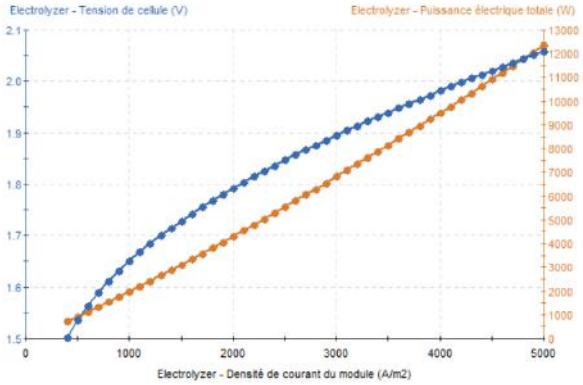

Fig.3: Cell voltage and total electrical power as a function of current density

In parallel, Figure 4 shows the relationship between the total electrical power input and the amount of heat exchanged. The results highlight the increasing thermal load on the system with higher current densities. This underscores the importance of effective thermal management to maintain safe and efficient operating conditions.

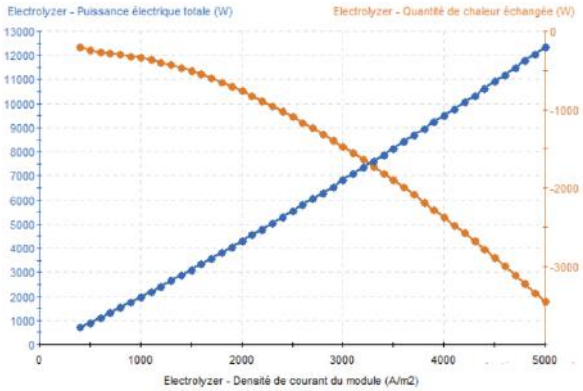

Fig.4: Total electrical power and exchanged heat as a function of current density

3.3. Hydrogen Production Simulation

3.3.1. Variation of Hydrogen Flow Rate with Electric Current

The hydrogen production rate was simulated across varying current densities, revealing different limiting regimes in the electrolysis process. These include: (1) the electron transfer-controlled regime, (2) the electrochemical reaction-controlled regime, and (3) the mass transfer-controlled regime. These regimes determine the kinetics and efficiency of hydrogen production. Industrial alkaline electrolyzers currently exhibit efficiencies up to 67%, and this study aims to computationally approach that benchmark.

As illustrated in Figure 5, the volumetric flow rate of hydrogen is directly proportional to the applied current. Additionally, the hydrogen output is influenced by the temperature of the alkaline solution. Higher temperatures enhance the reaction kinetics, thereby increasing hydrogen production. However, this is limited by the maximum operational temperature of 100°C in conventional alkaline electrolyzers.

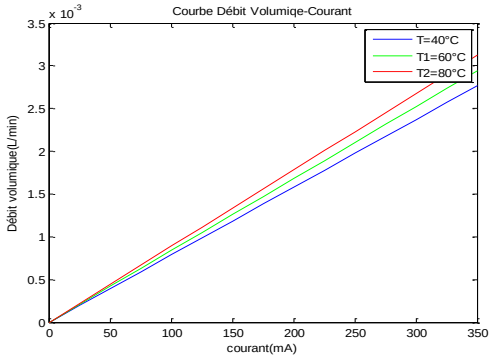

Fig.5: Volumetric hydrogen flow rate as a function of applied current

3.3.2. Hydrogen and Oxygen Production at the Electrodes

According to the simulation results summarized in Table 1, the production rates of hydrogen and oxygen at the electrodes show that the oxygen production rate is half that of hydrogen, consistent with stoichiometric expectations. A minor amount of hydrogen is also observed at the anode due to partial polarization of the electrolyte and electrode, suggesting some crossover or secondary electrochemical processes.

Table 1: Hydrogen and oxygen production rates at the electrodes

	At the anode	**At the cathode**	**Total**
hydrogen production amount	$0.02 Nm^3/h$	$1.97 Nm^3/h$	$1.99 Nm^3/h$
oxygen production amount	$0.99 Nm^3/h$	$0 Nm^3/h$	$0.99 Nm^3/h$

The molar composition of the final gas products is shown in Table 2. The hydrogen produced has a high purity level of 96.8%, which meets the requirements for many industrial applications, including fuel cell feeds and chemical synthesis.

Table 2: Molar fractions of hydrogen and oxygen in the final gas product

	Flow ($H_2 - OUT$)	**Flow ($O_2 - OUT$)**
Water	3.2%	3.2%
Hydrogen	96.8%	1.5%
Oxygen	0%	95.3%

Finally, the Faraday efficiency and total molar flow rate of hydrogen are plotted in Figure 6. The graph confirms a direct proportionality between hydrogen production and current density, indicating minimal parasitic reactions and confirming the reliability of Faraday's law in the studied range.

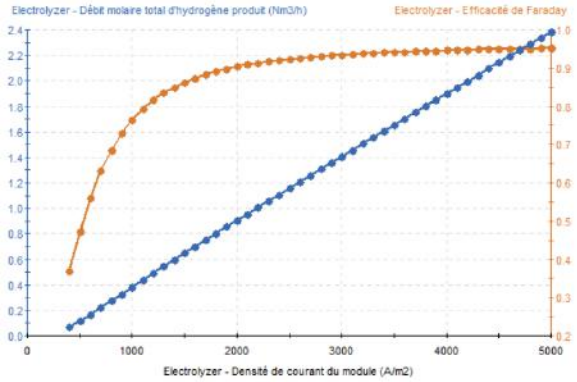

Fig.6: Total molar hydrogen production rate and Faraday efficiency as a function of current density

IV. CONCLUSION

In the pursuit of a low-carbon energy future, hydrogen has emerged as a central vector for decarbonizing hard-to-abate sectors and supporting the integration of variable renewable energy sources. However, the sustainability of hydrogen as an energy carrier fundamentally depends on the method of its production. This work contributes to that ambition by presenting a detailed and integrated mathematical model of alkaline water electrolysis, a mature, cost-effective, and scalable technology for green hydrogen generation. The proposed model addresses key aspects of electrolyzer performance by combining electrical, thermal, and electrochemical domains into a unified simulation framework.

The modeling results obtained through MATLAB/Simulink provide critical insights into how operating parameters influence the performance of the electrolyzer, particularly during the startup phase. The voltage-current characteristics show that increasing the electrolyte temperature leads to a decrease in operating voltage, primarily due to reductions in internal resistances and activation overpotentials. These findings emphasize the importance of thermal management in optimizing energy efficiency, as elevated temperatures facilitate faster reaction kinetics while simultaneously lowering the energy barrier for electrolysis. Therefore, managing heat flow within the system is not just a safety requirement, it is a design imperative for enhancing productivity and minimizing energy consumption.

A detailed decomposition of the total cell voltage into its fundamental components, reversible voltage, activation overpotential, ohmic loss, and concentration overpotential, offers a more precise understanding of the internal electrochemical processes. By explicitly modeling each loss mechanism, the study enables an accurate estimation of where energy is consumed or dissipated. This decomposition is especially useful for engineers and researchers aiming to design control strategies or advanced materials (e.g., low-resistance membranes, high-surface-area electrodes) that can mitigate specific inefficiencies and improve the overall energy yield of the system.

Sensitivity analyses conducted on current density variations further reveal nonlinear increases in both power consumption and heat generation at higher loads. These results underscore the necessity of balancing the gains in hydrogen production against potential losses in efficiency and system durability. As current density rises, the associated thermal and resistive burdens intensify, which, if unregulated, could compromise long-term stability. This trade-off between performance and thermal stress highlights the practical relevance of modeling not only for design purposes, but also for predictive maintenance, fault detection, and real-time process optimization.

Hydrogen production simulations further validate the model's consistency with Faraday's law, demonstrating a near-linear relationship between applied current and volumetric gas output. The purity level of hydrogen remains above 96%, confirming the suitability of alkaline electrolyzers for industrial applications such as fuel cell supply and chemical processing. Additionally, the stoichiometric ratio of hydrogen and oxygen production reflects sound mass balance, and minor deviations linked to parasitic effects such as crossover are quantitatively assessed. These results establish the credibility of the model for replicating real-world behavior and benchmarking system performance.

In summary, the developed electrochemical and thermal model offers a powerful and flexible tool for advancing green hydrogen technologies. By integrating diverse physical phenomena into a coherent simulation environment, it enables robust design, control, and scale-up of electrolyzer systems. Beyond scientific validation, this model serves a broader strategic goal: facilitating the deployment of renewable hydrogen infrastructure at both centralized and decentralized scales. As countries strive to meet climate targets and restructure their energy systems, such tools are indispensable for guiding investment decisions, improving system efficiency, and accelerating the global transition toward sustainable hydrogen production.

REFERENCES

[1] International Energy Agency (IEA). (2019). *The Future of Hydrogen: Seizing today's opportunities*. Report prepared by the IEA for the G20, Japan. https://www.iea.org/reports/the-future-of-hydrogen

[2] Hydrogen Council. (2020). *Path to hydrogen competitiveness: A cost perspective*. Retrieved from https://hydrogencouncil.com/en/path-to-hydrogen-competitiveness-a-cost-perspective/

[3] International Energy Agency (IEA). (2021). *Global Hydrogen Review 2021*. Paris: IEA. https://www.iea.org/reports/global-hydrogen-review-2021

[4] United Nations Framework Convention on Climate Change (UNFCCC). (2015). *The Paris Agreement*. Retrieved from https://unfccc.int/process-and-meetings/the-paris-agreement/the-paris-agreement

[5] [Carmo, M., Fritz, D. L., Mergel, J., & Stolten, D. (2013). A comprehensive review on PEM water electrolysis. *International Journal of Hydrogen Energy*, 38(12), 4901–4934. https://doi.org/10.1016/j.ijhydene.2013.01.151

[6] Millet, P., Grigoriev, S., Pinaud, N., Mbemba, N., Ranjbari, A., & Etievant, C. (2013). Power-to-gas: Electrolysis and methanation status review. *Renewable and Sustainable Energy Reviews*

[7] Zeng, K., & Zhang, D. (2010). *Recent progress in alkaline water electrolysis for hydrogen production and applications*. Progress in Energy and Combustion Science, 36(3), 307–326

[8] Atkins, P., & de Paula, J. (2010).*Atkins' Physical Chemistry* (9th ed.). Oxford University Press